

An improved method for separating the kinetics of anisotropic and topographic gratings in side-chain azobenzene polyesters

M. Helgert^{1,*}, B. Fleck¹, L. Wenke¹, S. Hvilsted², P.S. Ramanujam²

¹ Institut für Angewandte Optik, Friedrich-Schiller-Universität Jena, Fröbelstieg 1, 07743 Jena, Germany
(Fax: +49-3641/947-652, E-mail: helgert@pinet.uni-jena.de)

² Risø National Laboratory, Frederiksborgvej 399, P.O. Box 49, 4000 Roskilde, Denmark

Received: 27 October 1999/Revised version: 16 February 2000/Published online: 27 April 2000 – © Springer-Verlag 2000

Abstract. The induction of anisotropy gratings in side-chain azobenzene polyesters is accompanied by the formation of surface relief. We introduce an improved holographic method to separate the contributions of the anisotropic and the topographic part to the diffraction efficiency by analyzing the polarization of the first-order diffracted beam. The main advantage of this method is that both parts can be determined simultaneously by only one measurement. Furthermore the displacement between both gratings can be determined in a similar manner. Experimental results obtained with two different polyesters are presented.

PACS: 42.40.Lx; 42.65.Vh; 42.25.Ja

Since the first observation of surface relief formation in azobenzene polyesters due to irradiation with two coherent light waves [1, 2], this phenomenon has been the subject of a multitude of investigations [3–7]. The effect is of great interest concerning potential applications, for instance in the field of the fabrication of diffractive optical elements. Such elements could be produced without any wet processing by optical means exclusively. Therefore a better understanding of the basic processes and knowledge about the kinetic of the relief formation are necessary.

Under the influence of a polarized light wave the chromophore moieties in a photoanisotropic medium undergo trans-cis isomerization cycles, which lead to a reorientation of those molecules perpendicular to the direction of the field vector. The material becomes birefringent. A periodic field distribution, which can be obtained by coherent superposition of two orthogonal polarized light waves, can thus be inscribed in the bulk of such a material as a varying optical anisotropy. In azobenzene polymers the induction of such polarization gratings initiates the formation of surface relief gratings. The features of the reliefs are strongly dependent on the type of anisotropy grating in the bulk of the polymer material. It has

been established that the intensities and polarization states of the light waves producing the field modulations are strongly responsible for the nature of the surface relief. Also the polymer architecture has an essential influence.

A peculiarity of polarization gratings is the fact, that the diffraction efficiency and the polarization states of the diffracted beams are in general dependent on the polarization states of the recording beams and the readout beam as well. For example the first-order diffracted beam of a polarization grating produced with orthogonal circular polarized beams is always circularly polarized, independent of the polarization of the readout beam. In contrast for pure surface relief gratings the polarization of the diffracted beam would not be altered by the diffraction process. Considerations of this kind open possibilities to separate the contributions of both gratings to the diffraction by analyzing the polarization states of the diffracted orders.

Holme et al. developed a polarization holographic method to perform such a separation [8, 9]. Thereby the displacement between both gratings had been determined by a related method. In both cases the polarization of the first-order diffracted beam has been analyzed for different linearly polarized states of the readout wave. The final result was obtained by combination of data of at least two measurements. This could be problematic because of temporal fluctuations of the diffracted beams, which we have found to occur due to mechanical instabilities. Especially for measurements revealing the temporal behaviour of the relief formation such a combination of temporal uncorrelated data should be avoided. In this article we present a modified method that avoids this problem.

1 Theory

The method is based on the fabrication of a polarization grating that is accompanied by relief formation by coherent superposition of two beams polarized along $\pm 45^\circ$ with respect to the grating vector (x axis) which intersect in the plane of

*Corresponding author.

the sample under an angle of 2θ . The total field can be written in terms of a Jones vector for small intersection angles 2θ :

$$\begin{pmatrix} E_x \\ E_y \end{pmatrix} = \sqrt{I} \begin{pmatrix} \cos \delta \\ i \sin \delta \end{pmatrix}. \quad (1)$$

$\delta = \frac{2\pi}{\lambda} x \sin \theta$ is the phase across the film plane for the first recording beam, for the second beam it is $-\delta$, consequently the relative phase between both beams is 2δ . The total intensity I of the field in the film plane is constant but the polarization is modulated along the grating vector as depicted in Fig. 1. This modulation induces a continuously varying optical anisotropy with the optical axes parallel and perpendicular to the grating vector.

This anisotropy grating can be described in terms of a phase plate with spatially varying phase shift. It can be described by the following Jones matrix:

$$T_a = \begin{pmatrix} e^{i\Delta\phi \cos(2\delta)} & 0 \\ 0 & e^{-i\Delta\phi \cos(2\delta)} \end{pmatrix}. \quad (2)$$

The amplitude of the spatially varying relative phase shift of the phase plate is thus $2\Delta\phi$. Considering the effect of the surface relief grating there will be no relative phase shift between the x - and y -component of a probe beam but a spatially varying absolute phase shift for both components due to the thickness modulations. The Jones matrix describing the transmittance of the surface relief grating is thus given by

$$T_r = \begin{pmatrix} e^{i\Delta\psi \cos(2\delta+\delta_0)} & 0 \\ 0 & e^{i\Delta\psi \cos(2\delta+\delta_0)} \end{pmatrix}. \quad (3)$$

Here $\Delta\psi = \frac{2\pi}{\lambda} \Delta h(n_p - n_a)$, where $2\Delta h$ is the relief height and n_p and n_a are the refractive indices of the polyester and air. The constant δ_0 accounts for a possible displacement between the two gratings. A sinusoidal shape of the relief has been assumed in accordance with AFM scans performed previously [5, 9].

Now the diffraction of a probe beam by these gratings will be considered. We assume the anisotropic-topographic grating system to consist of the two gratings in succession. That means that the probe beam first passes the surface grating without anisotropy and then the pure anisotropy grating in the bulk. Therefore the total Jones matrix of the diffracting system is

$$T = T_a T_r. \quad (4)$$

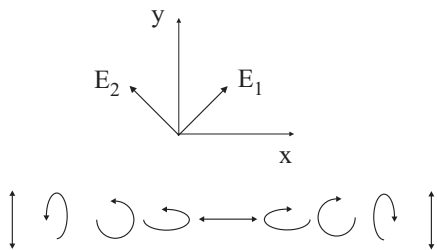


Fig. 1. Polarization of the recording beams and resulting modulation of the polarization state along the grating vector

In a straightforward calculation the matrix for the $+1$ order of diffraction

$$T_{+1} = \begin{pmatrix} A e^{i\delta_0} + B & 0 \\ 0 & A e^{i\delta_0} - B \end{pmatrix} \quad (5)$$

is obtained with

$$A = J_0(\Delta\phi) J_1(\Delta\psi) \quad (6)$$

and

$$B = J_0(\Delta\psi) J_1(\Delta\phi). \quad (7)$$

The J_i ($i = 0, 1$) are the zeroth and first-order Bessel functions of the first kind, the phase shifts $\Delta\phi$ and $\Delta\psi$ have been assumed to be small so that higher order terms are negligible.

It should be remarked, that in the Jones matrices T_a and T_r the absorbance of the material was neglected for simplification. This is justified because of the small absorbances of the samples used in our experiments at the wavelengths of the recording and reading beams which are given in Sect. 2.

First the displacement δ_0 between both gratings can be determined. For that purpose the polarization state of the readout beam with intensity I_0 was chosen to be right-handed circular, accordingly the wave in the $+1$ order is

$$E_{+1} = T_{+1} \sqrt{\frac{I_0}{2}} \begin{pmatrix} 1 \\ i \end{pmatrix} = \sqrt{\frac{I_0}{2}} \begin{pmatrix} A e^{i\delta_0} + B \\ i (A e^{i\delta_0} - B) \end{pmatrix}. \quad (8)$$

This diffraction order can be split (by means of a Wollaston prism) into a horizontal and a vertical polarized beam with intensities

$$I_{ch} = \frac{I_0}{2} |A e^{i\delta_0} + B|^2 = \frac{I_0}{2} (A^2 + B^2 + 2AB \cos \delta_0) \quad (9)$$

and

$$I_{cv} = \frac{I_0}{2} |A e^{i\delta_0} - B|^2 = \frac{I_0}{2} (A^2 + B^2 - 2AB \cos \delta_0). \quad (10)$$

The first index c indicates the circular polarization of the probe beam, the second one v, h refers to the vertical and horizontal components of the diffracted beam. From an experiment described by Holme [9] we know, that in these materials a linear polarized beam induces a birefringence with the fast axis in field direction ($\Delta\phi < 0$). This means that $A > 0$ and $B < 0$. Furthermore from symmetry considerations the value of δ_0 is expected to be only $0, \pm\frac{\pi}{2}$, or π . Lagugn  Labarthe et al. have discussed the possibility of the displacement being different from the above values [10–12]. This question will be treated at the end of this section. As a result of the calculation we see that by measuring the intensities I_{ch} and I_{cv} the phase shift between the two gratings can be determined. If $\delta_0 = 0$ then $I_{ch} < I_{cv}$ follows, that means that the peaks of the surface relief correspond to the horizontal polarization. For $\delta_0 = \pi$ in contrast $I_{ch} > I_{cv}$, the surface relief peaks occur on places with vertical polarization. For a phase shift of $\delta_0 = \pm\frac{\pi}{2}$ both intensities should be equal.

In the section describing the experimental part of this work we present results of the corresponding measurements on two different azobenzene polyesters. The advantage of this

method compared with that described in [8] is that by choosing circular polarization of the readout beam the result can be obtained by only one measurement.

In a similar way the method for the determination of $\Delta\phi$ and $\Delta\psi$ and their temporal behaviour [8] can be improved in the same sense by reading out that grating with $+45^\circ$ polarization and detecting the intensities of the components polarized in $+$ and -45° direction.

For that case the Jones vector of the beam diffracted into the first order is obtained by

$$E_{+1} = T_{+1} \sqrt{\frac{I_0}{2}} \begin{pmatrix} 1 \\ 1 \end{pmatrix} = \sqrt{\frac{I_0}{2}} \begin{pmatrix} A e^{i\delta_0} + B \\ A e^{i\delta_0} - B \end{pmatrix}. \quad (11)$$

Now this order is split into the components polarized in $+45^\circ$ and -45° direction, for that case in the experiment the Wollaston prism has to be rotated by an angle of 45° . In the calculation we first consider the first component, which is found by multiplication of the Jones vector of the diffracted beam (11) with the Jones matrix of a linear polarizer with the axis in $+45^\circ$ direction:

$$\begin{aligned} E_{+1}^{+45^\circ} &= \frac{1}{2} \begin{pmatrix} 1 & 1 \\ 1 & 1 \end{pmatrix} \sqrt{\frac{I_0}{2}} \begin{pmatrix} A e^{i\delta_0} + B \\ A e^{i\delta_0} - B \end{pmatrix} \\ &= A e^{i\delta_0} \sqrt{\frac{I_0}{2}} \begin{pmatrix} 1 \\ 1 \end{pmatrix}. \end{aligned} \quad (12)$$

The measured intensity of that component is therefore

$$I_{+1}^{+45^\circ} = I_0 A^2 = I_0 [J_0(\Delta\phi) J_1(\Delta\psi)]^2. \quad (13)$$

In the analogous way the component polarized in the -45° direction is calculated to be

$$I_{+1}^{-45^\circ} = I_0 B^2 = I_0 [J_0(\Delta\psi) J_1(\Delta\phi)]^2. \quad (14)$$

These intensities are independent of the phase shift δ_0 but dependent on the amounts of $\Delta\phi$ and $\Delta\psi$. Hence the contributions of the anisotropy grating and the surface relief to the diffraction can not be separated exactly by measuring these intensities. But appropriate approximations deliver good results with sufficient accuracy.

For small values of $\Delta\phi$ and $\Delta\psi$ the approximation

$$J_0(\Delta\phi) \approx J_0(\Delta\psi) \approx 1 \quad (15)$$

is valid, as for example $J_0(0.3) \approx 0.98$. Furthermore the expansion of the first-order Bessel function shows that

$$J_1(\Delta\phi) \approx \frac{\Delta\phi}{2}; \quad J_1(\Delta\psi) \approx \frac{\Delta\psi}{2} \quad (16)$$

are good approximations too. So for instance $J_1(0.3) \approx 0.148$.

Consequently from (13) and (14) one gets the final expressions

$$\Delta\phi \approx 2\sqrt{\frac{I_{+1}^{-45^\circ}}{I_0}}; \quad \Delta\psi \approx 2\sqrt{\frac{I_{+1}^{+45^\circ}}{I_0}} \quad (17)$$

for the experimental determination of the phase shifts by measuring the intensities of the beams behind the Wollaston prism.

The curves $\Delta\phi(t)$ and $\Delta\psi(t)$ obtained in this way are independent of the phase shift δ_0 between both gratings. Formally it would be possible to calculate $\delta_0(t)$ by inserting $\Delta\phi(t)$ and $\Delta\psi(t)$ into (9) or (10). Therefore the necessary data $I_{ch}(t)$ and $I_{cv}(t)$ must be obtained under the same experimental conditions as $\Delta\phi(t)$ and $\Delta\psi(t)$. That would be related to the calculations presented in [11] leading to displacements δ_0 different from that assumed by symmetry considerations we made.

2 Materials

In the experiments two different types of azobenzene polymers were used. The structural formulas are given in Fig. 2. The first used polymer was a liquid crystalline polyester with the abbreviation P6a12. The second was an amorphous azobenzene side-chain polyester denoted E1aP.

The substantial difference between both polymers is the existence of an aromatic ring in E1aP resulting in a stiffened main-chain. Both polyesters contain cyanoazobenzene in the side-chains. P6a12 has a hexamethylene spacer with a dodecamethylene sequence in the main-chain. E1aP has one methylene spacer with a partial aromatic main-chain. The preparation of P6a12 is described in [13] where a glass transition at 24°C was specified. The sample used in our investigations had a number-averaged molecular mass M_n of 27 000 and a corresponding weight-averaged molecular mass M_w of 72 000 as determined by size exclusion chromatography (SEC) with polystyrene standards calibration. E1aP is prepared in a similar way through melt transesterification of 3-[4-((4-cyanophenyl)azo)-phenoxy]-1,2-propanediol and diphenyl phthalate. The diol is synthesized by means of a base catalyzed coupling of 4-[4-(cyanophenyl)azo]-phenol and 3-bromo-1,2-propanediol. E1aP has a M_n of 7900 and a M_w of 11 800. A differential scanning calorimetry (DSC) analysis discloses E1aP as an amorphous material with a glass transition at 107°C .

In the experiment an argon laser at 514.5 nm was used for recording and a He-Ne laser beam (633 nm) for reading out. The absorbance of both samples at 514.5 nm is less than 0.05 and less than 0.01 at 633 nm. The thicknesses of the samples were approximately 2 μm .

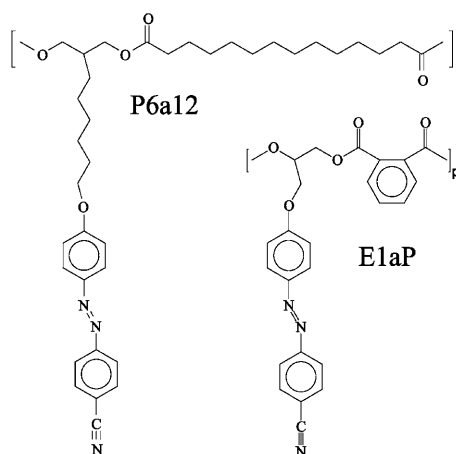


Fig. 2. Chemical structures of E1aP and P6a12

3 Experiment

The setup used for the experimental realisation of the method described above is shown in Fig. 3.

The polarization states of the recording beams (514.5 nm) were adjusted in $\pm 45^\circ$ directions by linear polarizers. The angle θ was approximately 5° , which is small enough to justify the application of the Jones calculus to determine the field distribution. The HeNe probe beam at 633 nm was circularly polarized by a quarter-wave plate for the determination of the phase shift δ_0 between both gratings. For the second part of the experiment, the measurement of $\Delta\phi$ and $\Delta\psi$, the quarter-wave plate has been removed and the probe beam was linear polarized in $+45^\circ$ direction. The light diffracted in the $+1$ order was split by a Wollaston prism into the horizontal and vertical polarized components. The corresponding intensities were measured by two photodetectors. In the second part this prism has been rotated by 45° in accordance with the above calculation.

In Figs. 4 and 5 the results concerning the phase shift δ_0 for both polymers are presented. The grating was recorded (start at $t = 10$ s) for 120 s with a total intensity of 350 mW/cm^2 of the argon laser beams. The illumination was stopped at $t = 130$ s. The intensity of the readout HeNe laser beam was 0.9 mW/cm^2 .

Obviously the polymers P6a12 and E1aP show exactly the opposite behaviour. For P6a12 the curves (Fig. 4) reveal that $I_{\text{ch}} < I_{\text{cv}}$, so $\delta_0 = 0$ and the peaks of the surface relief correspond to the horizontal polarization. In E1aP the peaks form up on places with vertical polarization as can be concluded from Fig. 5. It is remarkable that these results have been predicted by considerations concerning the surface relief formation on the basis of light-induced shape changes that are described elsewhere [14].

The occurrence of temporal fluctuations of the detected intensities is believed to be due to mechanical instabilities. As can be seen from Figs. 4 and 5 both polyesters display a quite different behaviour in this regard. For P6a12 the fluc-

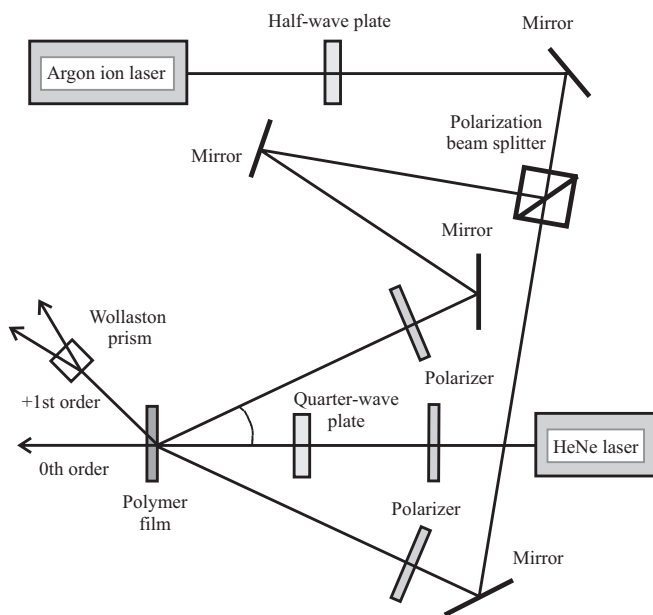


Fig. 3. Experimental setup

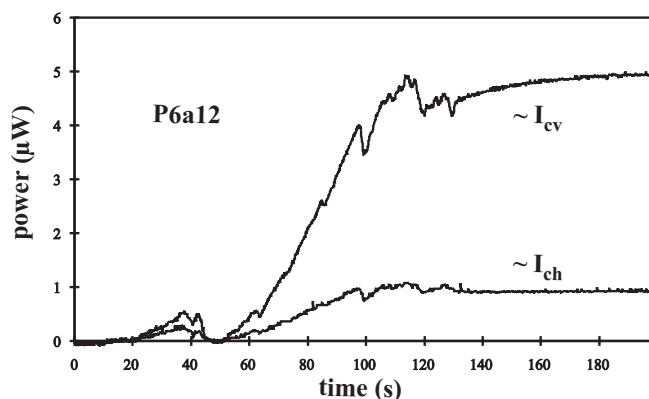


Fig. 4. Experimental curves I_{ch} and I_{cv} as functions of time for P6a12

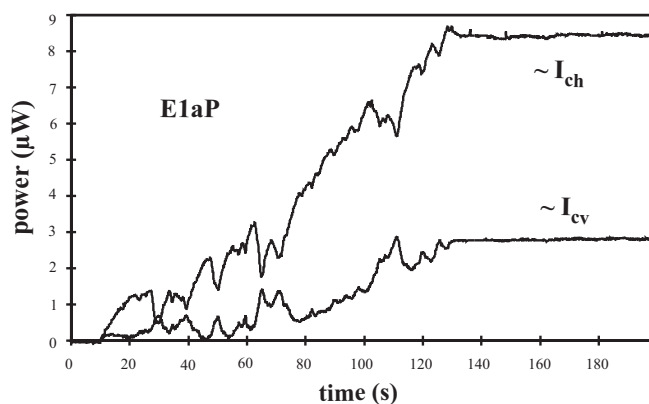


Fig. 5. Experimental curves I_{ch} and I_{cv} as functions of time for E1aP

tuations appear synchronously in both components I_{cv} and I_{ch} whereas for E1aP a decrease in the horizontal component correlates with an increase of the vertical one and vice versa. This behaviour can be understood by taking into account the different time constants for the induction of an anisotropy by a single argon laser beam. In that case we found for a laser intensity of about 350 mW/cm^2 that the process in P6a12 is clearly slower than in E1aP. In P6a12 80% of the saturation value is reached after 30 s of irradiation, whereas in E1aP this is already accomplished after approximately 2 s.

If as a result of a mechanical concussion the field distribution is shifted against the sample with a certain amount of induced anisotropy and an advanced stage of relief formation, the orientational distribution of the chromophores will be altered. Depending on the duration of the displacement and the response time of the material the anisotropy at a certain place of the sample will first be diminished due to reinclusion of oriented chromophores in the isomerization cycles. Finally a new anisotropy will be induced with a different direction of the optical axis. In general the statistical shifts between the field distribution and the sample are short-time. In P6a12 only a temporary small decrease of the anisotropy results from that without the induction of a new shifted anisotropy grating, so only a decrease of the diffraction efficiency is observed simultaneously for both the horizontal and the vertical component. In E1aP the photoresponse is so fast that the shifted field distribution is nearly immediately transformed into a new anisotropy grating that will be shifted to the surface relief. But this phase shift dictates the ratio of the intensities I_{cv} and

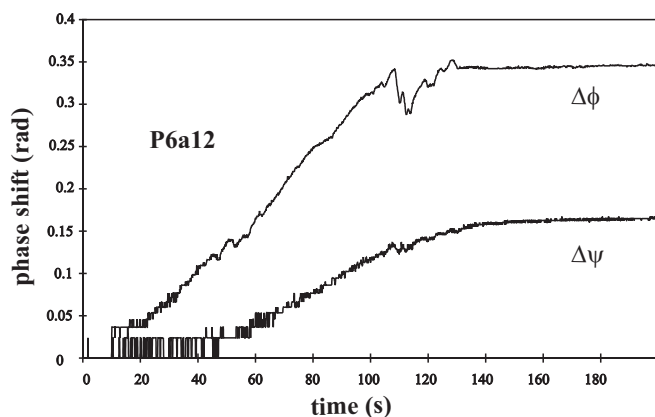


Fig. 6. Experimental curves $\Delta\phi$ and $\Delta\psi$ as functions of time for P6a12

I_{ch} as outlined in the theoretical section. For example a phase shift of $\pi/2$ means that $I_{cv} = I_{ch}$ (9) and (10). In our measurement this situation is reached at about $t = 30$ s (Fig. 5). From that consideration can be concluded that the amplitude of the temporal shifts due to mechanical instabilities must be in the magnitude of a quarter grating period ($\Lambda \approx 3$ μm), and therefore smaller than 1 μm .

The results of the measurements for the determination of the temporal behaviour of the induction of the anisotropy and the relief formation are shown in Figs. 6 and 7. The values for $\Delta\phi$ and $\Delta\psi$ were obtained corresponding to (17). Again the exposure was started at $t = 10$ s and stopped at $t = 130$ s. The laser intensities were as specified above.

The curves reveal the different temporal behaviour of the induction of the anisotropy grating and the relief formation. In E1aP the latter process is clearly slower, whereby the phase shift due to the surface relief (≈ 0.35) exceeds the one caused by the anisotropy (≈ 0.1). In other words, for short exposure times the anisotropic grating dominates, only to be exceeded by surface relief for larger times. This fits well with observations in other amorphous polymers [15, 16]. In P6a12 both processes are slower than in E1aP, here $\Delta\phi$ (≈ 0.35) dominates in comparison with $\Delta\psi$ (≈ 0.15). Using the definition $\Delta\psi = \frac{2\pi}{\lambda} \Delta n \Delta h$, the relief height $2\Delta h$ corresponding to a $\Delta\psi$ of 0.35 is in the range of 50 nm, which is a typical value for surface reliefs in these materials under the mentioned experimental conditions and proves the applicability of the introduced method. An interesting detail is that the formation of the surface relief stops in the absence of the argon laser irradiation, though the saturation value of the optical anisotropy has been reached before (in Figs. 6 and 7 at $t = 130$ s). This observation should be the subject of further investigations.

4 Conclusions

A holographic method for the determination of the phase shift between the anisotropy grating and the surface relief and for

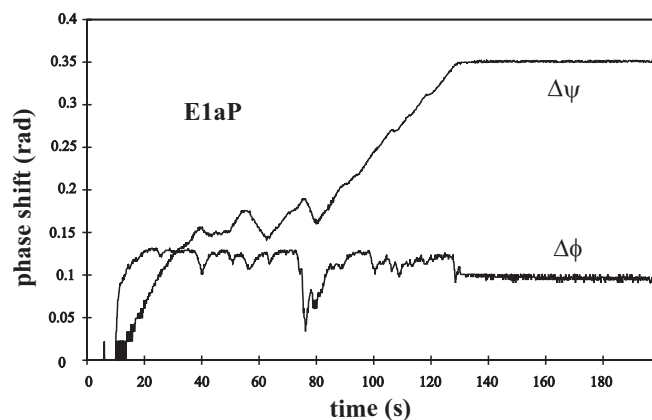


Fig. 7. Experimental curves $\Delta\phi$ and $\Delta\psi$ as functions of time for E1aP

the measurement of the temporal behaviour of the respective contributions to the diffraction has been presented. It was demonstrated, that occurring temporal fluctuations caused by mechanical instabilities have no disturbing impact on the results because by a proper choice of the polarization states of the acting waves all relevant quantities can be measured simultaneously. Experimental results obtained with two different azobenzene polyesters have been presented. We believe that this method can be helpful for further investigations of the dynamic of the surface relief formation in these materials.

References

1. P.L. Rochon, E. Batalla, A. Natansohn: Appl. Phys. Lett. **66**, 136 (1995)
2. D.Y. Kim, S.K. Tripathy, L. Li, J. Kumar: Appl. Phys. Lett. **66**, 1166 (1995)
3. C. Barrett, A.L. Natansohn, P.L. Rochon: J. Phys. Chem. **100**, 8836 (1996)
4. P. Lefin, C. Fiorini, J.M. Nunzi: Pure Appl. Opt. **7**, 71 (1998)
5. T.G. Pedersen, P.M. Johansen, N.C.R. Holme, P.S. Ramanujam, S. Hvilsted: Phys. Rev. Lett. **80**, 89 (1998)
6. J. Kumar, L. Li, X.L. Jiang, D.Y. Kim, T.S. Lee, S. Tripathy: Appl. Phys. Lett. **72**, 2096 (1998)
7. I. Naydenova, L. Nikolova, T. Todorov, N.C.R. Holme, P.S. Ramanujam, S. Hvilsted: J. Opt. Soc. Am. B **15**, 1257 (1998)
8. N.C.R. Holme, L. Nikolova, P.S. Ramanujam, S. Hvilsted: Appl. Phys. Lett. **70**, 1518 (1997)
9. N.C.R. Holme: Ph.D dissertation, Risø (1997)
10. F. Lagugné Labarthe, T. Buffeteau, C. Sourisseau: J. Phys. Chem. B **103**, 6690 (1999)
11. F. Lagugné Labarthe, T. Buffeteau, C. Sourisseau: J. Phys. Chem. B **102**, 2654 (1998)
12. F. Lagugné Labarthe, T. Buffeteau, C. Sourisseau: J. Phys. Chem. B **102**, 5754 (1998)
13. S. Hvilsted, F. Andruzzi, C. Kulinna, H.W. Siesler, P.S. Ramanujam: Macromolecules **28**, 2172 (1995)
14. D. Bublitz, M. Helgert, B. Fleck, L. Wenke, S. Hvilsted, P.S. Ramanujam: DOI 10.1007/s003400000281
15. N.C.R. Holme, L. Nikolova, T.B. Norris, S. Hvilsted, M. Pedersen, R.H. Berg, P.H. Rasmussen, P.S. Ramanujam: Macromol. Symp. **137**, 83 (1999)
16. F. Andruzzi, A. Altomare, F. Ciardelli, R. Solaro, S. Hvilsted, P.S. Ramanujam: Macromolecules **32**, 448 (1999)